

## STUDY ON THE INFLUENCE OF REMANENCE ON SUSPENSION CONTROL OF MAGNETIC SUSPENSION ROTOR

Jing FU<sup>1,\*</sup>, Xianfu LI<sup>2</sup>

*Ferromagnetic material itself has hysteresis property, which produces remanence in some applications. Through practical cases, this study analyzes the influence of residual magnetism on the suspension of magnetic suspension rotor during operation. Firstly, the causes of remanence are explained. Secondly, the remanence is simulated by permanent magnet, and the experiment of remanence affecting the suspension of magnetic suspension rotor is carried out, the results of which are compared with the simulation. Finally, the relationship among remanent magnetic field, magnetic suspension bearing control magnetic field and air gap is studied, and the critical value of ratio of remanent magnetic field to control magnetic field is obtained under different air gaps. By modifying the structure and material of magnetic suspension rotor in actual cases, the influence of residual magnetism on the suspension of magnetic suspension rotor is avoided, and the correctness of the study is verified.*

**Keywords:** magnetic suspension rotor, magnetic bearing, residual magnetism, critical value

### 1. Introduction

Magnetic bearing [1] is a kind of high-performance mechatronics bearing using electromagnetic force to suspend the supported parts stably in space, which has the advantages of no contact, no lubrication, no wear, no seal and so on and is widely used in military industry, ultra-clean environment, machine tools, computer equipment and many other fields. In some applications, magnetic suspension rotors need high-strength materials, but the hysteresis characteristics [2] of some high-strength materials are evident, producing large remanence in operation and affecting the stable operation of magnetic bearings. In such cases, it is necessary to study the influence of magnetic bearing remanence. At present, most of the domestic and foreign researches on remanence are aimed at the remanence of power transformer core [3]. In 2009, Feng Yuancheng et al. [4] analyzed the production mechanism of transformer remanence and the influence

<sup>1</sup> School of Mechanical and Electronic Engineering, Henan Institute of Technology, Xinxiang, Henan, China

<sup>2</sup> School of Mechanical and Electrical Engineering, Wuhan University of Technology, Wuhan, Hubei, China

of remanence on equipment operation with some countermeasures. In 2011, Xing Yunmin proposed a method to estimate the remanence of transformer core to work out the remanence in the core after transformer trips [5]. 2014 Markus Pütter et al. [6] discussed the effect of remanence on several diagnostic measuring methods and excitation surge current, introducing how to use mobile test equipment to overcome on-site degaussing. In 2016, Xu Xingshuai [7] analyzed the causes of remanence produced by power transformer core, expounded the possible harm, and explored the effective detection methods to reduce the core remanence. The paper will carry out the relevant research on the influence of remanence on the suspension control of magnetic suspension rotor based on an actual case.

## 2. Influence of Remanence on Suspension Control of Magnetic Suspension Rotor

The rotor material is 38CrMoAl, and Fig. 1 is the schematic diagram of its structure. The magnetic suspension rotor is debugged by proportional-integral-derivative control. During the debugging, the rotor cannot be suspended normally, and the current of the left and right coils on the axial magnetic bearing is shown in Fig. 2.

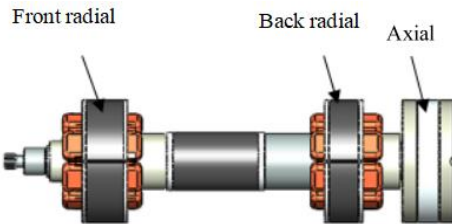


Fig. 1. Structure Diagram of the Magnetic suspension rotor

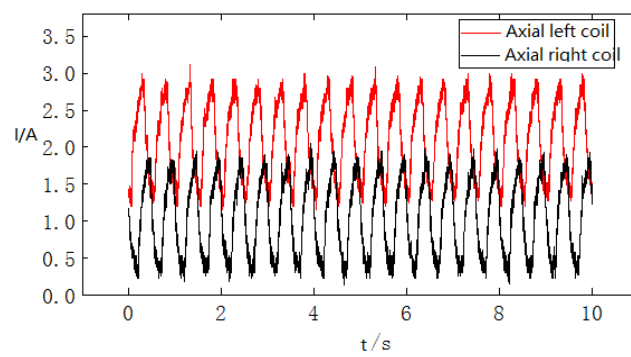


Fig. 2. Current of the Left and Right Coils of Axial Magnetic Bearing

Referring to the basic theory of magnetic suspension [8] and the symmetry of axial magnetic bearing, the current of the left and right coils should be similar

when it is stably suspended, but it is observed from Fig. 2 that the current is vastly different, and the rotor cannot be stably suspended. At this point, the axial displacement is shown in Fig. 3.

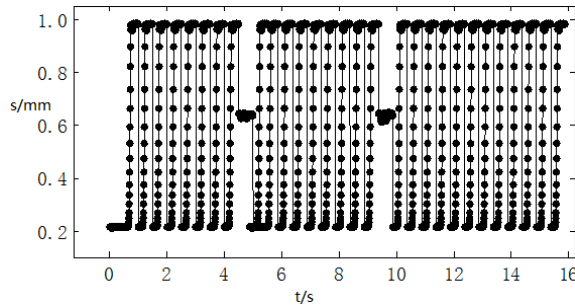
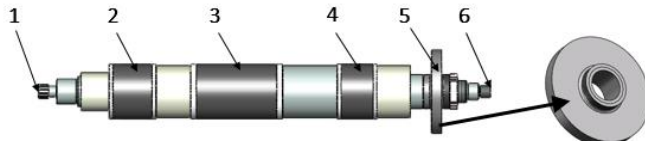


Fig. 3. Output Displacement Waveform of the Axial Sensor

As can be seen from Fig. 3, the rotor has runout on the left and right ends, that is, the magnetic suspension rotor collides with the axial protection bearing left and right, with only a transient suspension in the middle, but it soon becomes unstable. As the debugging stops, the rotor obviously has remanence. The rotor structure is shown in Fig. 4. After the rotor is placed for different time periods, the magnetic flux density of each surface is measured by Gauss meter.



1: Front end face; 2: Front radial bearing rotor; 3: Motor rotor; 4: Rear radial bearing rotor; 5: Axial thrust plate; 6: Rear end face

Fig. 4. Structure Diagram of Rotor

The measured values are shown in Table 1:

*Table 1*  
**Measured values of magnetic flux density (mT) after the rotor has been placed for different time periods**

Shaft Section	Placement Period After 0.5h	Placement Period After 3h	Placement Period After 24h
1	2.8	2.8	1.2
2	1.2	1.1	0.5
3	1.4	1.4	0.5
4	3.4	3.2	1.5
5	17.8	12.3	4.9
6	12.8	11.5	2.5

It is observed from the Table that there is a strong remanence on each surface of the magnetic suspension rotor, thus it is speculated that the remanence may have an impact on the suspension control of the rotor. Next correlated analysis will be made specific to this speculation.

### 3. Analysis of the Generation Principle of Rotor Remanence

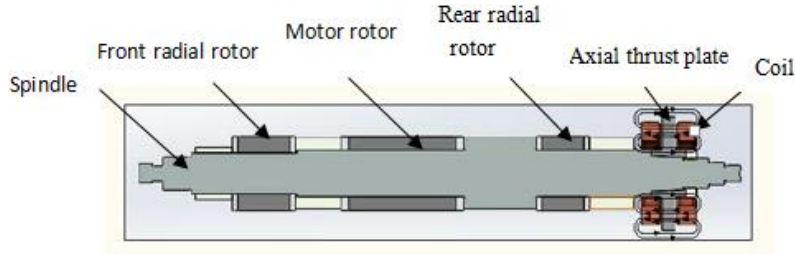


Fig. 5. Section View of Magnetic suspension rotor

The section view of the magnetic suspension rotor is shown in Fig. 5. The material of axial thrust plate is 42CrMo. From *Manual of Magnetic Characteristic Curves of Commonly Used Steel* [9], it is known that the hysteresis characteristic of CrMo steel is evident, as shown in Fig. 6.

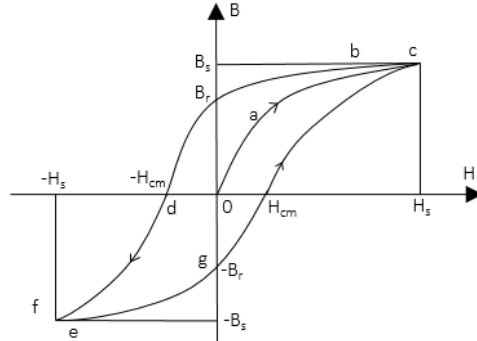


Fig. 6. Magnetic hysteresis loop of CrMo steel

Therefore, after the axial magnetic bearing coils are energized, the thrust plate will be excited, and the thrust plate will still have remanence after the coil is outage. There must be magnetic leakage flux in the transfer of magnetic remanence, so the transfer from 5→4→3→2 basically shows a decreasing trend. Because the relationship between the magnetic flux  $\Phi$  and the magnetic flux density  $B$  is

$$\phi = B \bullet S \quad (1)$$

In Formula (1),  $S$  is the distribution area of magnetic flux, while the area of Front end face 1 and Rear end face 6 is very small, and the flux density is large. Rear end face is closer to the thrust plate, and the magnetic leakage flux is relatively

less in the process of transfer, so the remanence of Rear end face is larger than that of Front end face.

#### 4. Comparison between Experiment and Simulation of Permanent Magnet Simulating Remanence

Because the remanence mainly comes from axial magnetic bearing, the bearing is specially studied below with the experimental principle as shown in Fig.7.

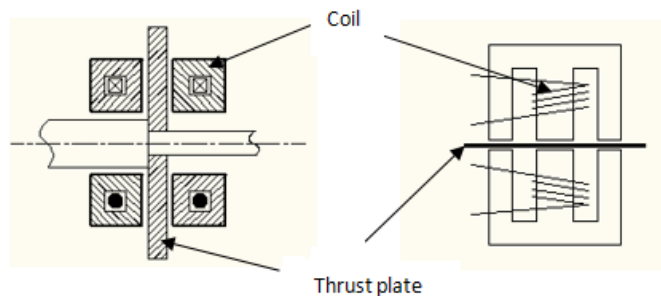


Fig. 7. Working Principle Diagram of the Experimental Device of Axial Magnetic Bearing

Because the thrust plate of the test device is of silicon steel sheet with good demagnetization, permanent magnets are used to simulate the existence of remanence. Fig. 8 and Fig.9 show the schematic diagram and three-dimensional model diagram of the experimental device respectively:

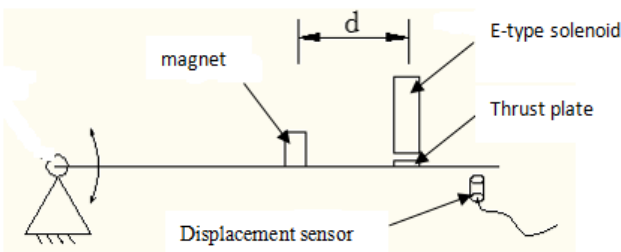


Fig. 8. Diagram of the Experimental Device

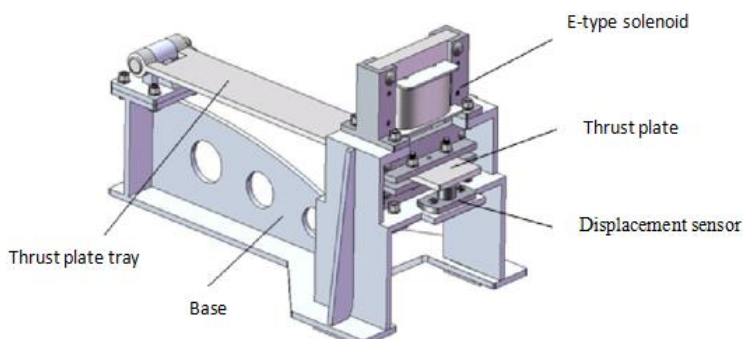


Fig. 9. Three-dimensional Model Diagram of the Experimental Device

Assuming that the air gap between the rotor core and the stator core is  $x_0$  when they are in equilibrium, the force relationship of the rotor core in the vertical direction is as follows(2)

$$p(t) + F_{mag} - mg = m \frac{d^2x}{dt^2} \quad (2)$$

Formula:  $p(t)$  is the disturbing force on the rotor in  $x$  direction;

$F_{mag}$  is the electromagnetic force of the magnetic bearing rotor;  
 $mg$  is the gravity of the rotor core.

$p(t)$  includes  $F_r$ (magnetic force of remanence) and  $F$ (other disturbing force). Compared with the magnetic force  $F_r$  of remanence, the force  $F$  produced by other factors (such as temperature, humidity and other environmental factors) can be neglected. Therefore, equation (2) can be written as

$$F_{mag} + F_r - mg = m \frac{d^2x}{dt^2} \quad (3)$$

From Maxwell's suction formula

$$F_{mag} = \frac{B^2 S}{2\mu_0} \quad (4)$$

$$F_r = \frac{B_r^2 S}{2\mu_0} \quad (5)$$

Formula :  $B$  is the magnetic induction intensity produced by electromagnet;

$B_x$  is the magnetic induction intensity corresponding to the remanence;

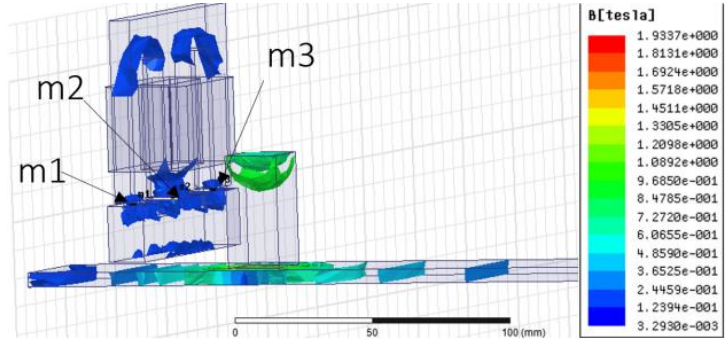
$S$  is the magnetic pole area;

$\mu_0$  is the air permeability;

Therefore, equation (3) can be changed into:

$$\frac{S}{2\mu_0} (B^2 + B_r^2) - mg = m \frac{d^2x}{dt^2} \quad (6)$$

The remanence simulation is that when it is not electrified, a permanent magnet is placed at the distance  $d$  from the E-shaped electromagnet (Fig. 8), and the magnetic flux density between the air gap is regarded as remanence. Fig. 10 is the simulation result of the magnetic flux density generated by permanent magnet when  $d = 2$  cm.

Fig. 10. Simulated Remanence at  $d = 2$  cm

The magnetic flux density values (that is, simulated remanence) at the three magnetic poles m1, m2 and m3 of the E-shaped electromagnet in Fig. 10 are shown in Table 2.

Table 2

Remanence values (mT) of the experimental device at  $d = 2$  cm

E-shaped Ferromagnetic Pole	m1	m2	m3
1	1	1	1
B	06.2	09.5	06.3

To verify the accuracy of remanence simulation, the results of remanence simulation and remanence simulation experiment are compared when  $d$  is 2 cm, 4 cm, 6 cm, 8 cm, 10 cm and 12 cm respectively. Because the magnetic flux density values of the three magnetic poles m1, m2 and m3 are basically the same, to compare the experimental values and simulation values further, Fig. 11 only compares the experimental and simulation values of the magnetic flux density at the middle magnetic pole m2. The results are shown in Fig. 11. It can be seen that the simulated remanence simulated values corresponding to different  $d$ s are basically consistent with the remanence simulation experimental values, indicating that the remanence simulated by permanent magnet is feasible. In the subsequent sections, the remanence values measured by experiments will be used for calculation.

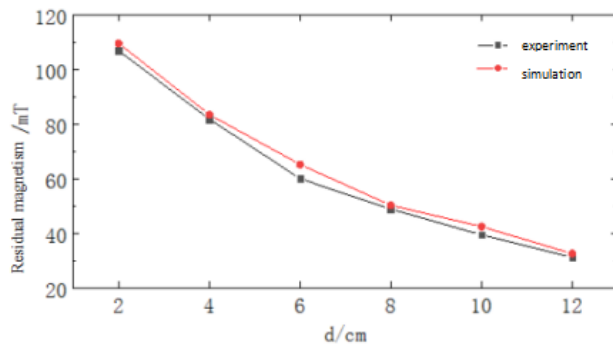


Fig. 11. Experimental and Simulated Values of Simulated Remanence under Different Distances

## 5. Effect of Remanence on the Suspension of Magnetic Suspension System

### 5.1 Effect of Remanence on the Suspension of Magnetic Suspension Rotor

To study the influence of remanence on magnetic bearing, the experimental device is connected with the Dspace [10,11] software and MATLAB program block diagram enabled, the parameters set, and the control desk software matched with Dspace is operated. The output voltage of the displacement sensor used is 0-5V with a linear range of 2mm. The sensor is calibrated before the experiment. When the distance between the sensor probe and the detection surface is 1.815mm, the output voltage is 0V; when the sensor probe is 3.843 mm away from the detection surface, the output voltage is 5V. The sensor is approximated as a linear element, and the fitting straight-line equation between the sensor detected value and the output voltage is  $U=2.4655D-4.475$ , ( $U$  is the output voltage of the sensor,  $V$ ;  $D$  is the actual distance between the probe and the thrust plate, mm). As the thrust plate is toggled to the position in contact with the lower protection bearing, the control desk software displays a distance of 2mm. As the thrust plate is toggled to the position in contact with the upper protection bearing with a distance of 3.4 mm and the thrust plate is suspended in the middle when  $D = 2.7$  mm, the voltage value is 2.18V. Because the displacement voltage signal detected by the sensor is input to the controller in line with the ratio of 10:1, the reference value of the equilibrium position is set to 0.218 V. The proportional-integral-derivative control parameters are adjusted next to make the thrust plate suspend stably at the equilibrium point, while finally the operation data for a period of time are recorded. Fig. 12 shows the output waveform of the eddy current displacement sensor as the magnetic bearing is suspending stably.

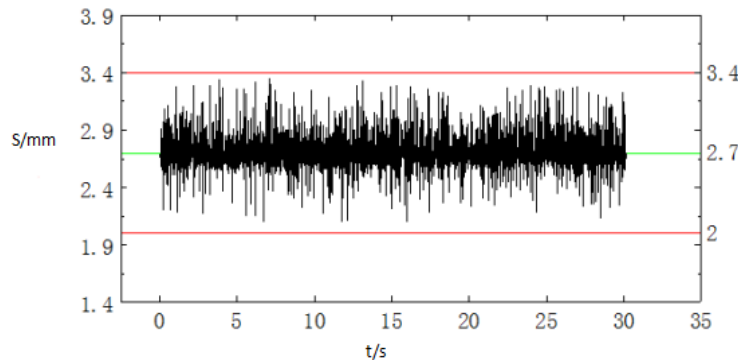


Fig. 12. Output Displacement Waveform of Sensor under Stable Suspension

The maximal air gap between the E-shaped iron and the thrust plate is 1.4mm. It is observed from Fig. 13 that the thrust plate floats at the equilibrium point and maintains stable suspension.

When the parameters are kept unchanged and the experimental device is operated again, following a few seconds of stable suspension of the thrust plate, an 800 mT permanent magnet is used to simulate the remanence, which is placed horizontally 2 cm away from the E-shaped iron (that is,  $d = 2$  cm), and the output waveform of the displacement sensor shown in Fig. 12 is obtained.

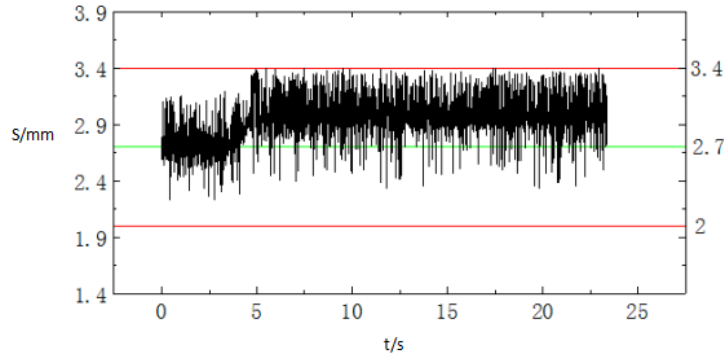


Fig. 13. Output Displacement Waveform of the Sensor at  $d = 2$  cm

It is seen from Fig. 13 that when the thrust plate is stably suspended, a permanent magnet is placed 2cm away from the E-shaped iron, the thrust plate changes from stable suspension into continuous collision with the upper protection bearing of the device, indicating that the thrust plate has become unstable. It has previously analyzed that remanence will have an impact on magnetic bearing, then it is necessary to analyze the influence degree of remanence on magnetic bearing. In addition, the maximal remanence without an impact on the suspension control of magnetic bearing is obtained through experiment.

Proportional-integral-derivative control parameters are adjusted to make the thrust plate suspend stably, and the magnetic flux density on the stator surface produced by control is measured as 281 mT by Gauss meter. A permanent magnet with a surface magnetic flux density of 800 mT is placed at different positions from the E-shaped iron to simulate different remanence. The distance values are 4 cm, 6 cm, 8 cm, 10 cm and 12 cm respectively, and the output displacement waveform of the displacement sensor similar to Fig. 12 is obtained.

However, as the permanent magnet is getting farther and farther away from the iron core, the influence on the suspension stability of the armature becomes smaller and smaller, and the stability is almost not affected when the permanent magnet is 12 cm away from the E-shaped iron. The phenomenon in the experiment is shown in Fig. 14.

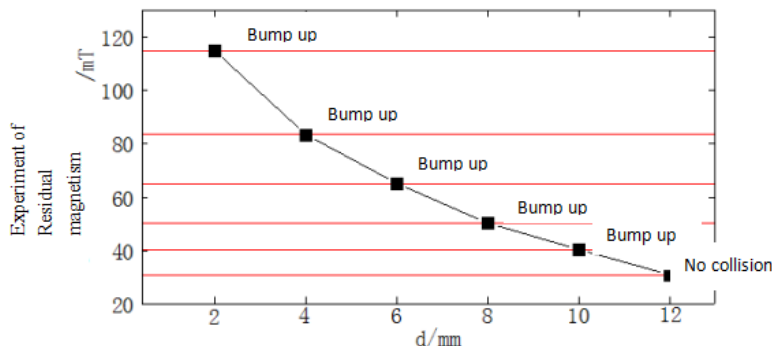


Fig. 14. Thrust Plate Collisions at Different Distances

Therefore, the distance of 12 cm is set as the critical point with no impact on its stability. The magnetic flux density between the air gaps of the experimental device is 31 mT as measured by Gauss meter. For the ease of calculation, the formula is defined as below

$$q_x = \frac{a}{b} \times 100\% \quad (7)$$

In formula (7):

*a* is the surface remanence of the thrust plate measured through the experiment;  
*b* is the magnetic flux density of the controlled magnetic field between the air gaps measured through the experiment;

*q<sub>x</sub>* indicates the critical value of suspension control that is not affected by the remanence when the air gap is *x*.

Therefore, if the air gap between the stator and rotor is 0.7mm, the critical value when remanence does not affect the suspension control is:

$$q_x = \frac{31}{287} \times 100\% = 10.8\%.$$

Below this value, the remanence has a slight effect on the suspension of the magnetic bearing, but it does not affect the stable suspension.

## 5.2. Effect of remanence on magnetic suspension rotor with different air gaps

The air gap between the stator and rotor of the magnetic suspension rotor axial magnetic bearing shown in Fig. 1 is 0.4 mm respectively on the left and right, and 10.8% obtained in the experiment is the result when the air gap is 0.7 mm. Therefore, to judge whether the remanence has an effect on its suspension control, the ratio must be obtained through experiment when the air gap between the stator and the rotor thrust plate is 0.4mm. Due to the measuring range of the displacement sensor of the experimental device, the air gap of 0.4 mm is difficult to suspend. Therefore, we use the same experimental method to obtain that the remanence that affects the suspension control of experimental device is 35 mT

when the air gap is 0.8 mm, and the magnetic flux density between the air gap is 285 mT in case of stable suspension when  $q_x = \frac{35}{285} \times 100\% = 12.3\%$ . At this time, it can also be arrived that when the air gap between the stator and rotor is 0.6 mm,  $q_x = \frac{26}{293} \times 100\% = 8.87\%$ . The  $q$  value fitted in case of air gaps 0.6 mm, 0.7 mm and 0.8 mm is as shown in Fig. 15.

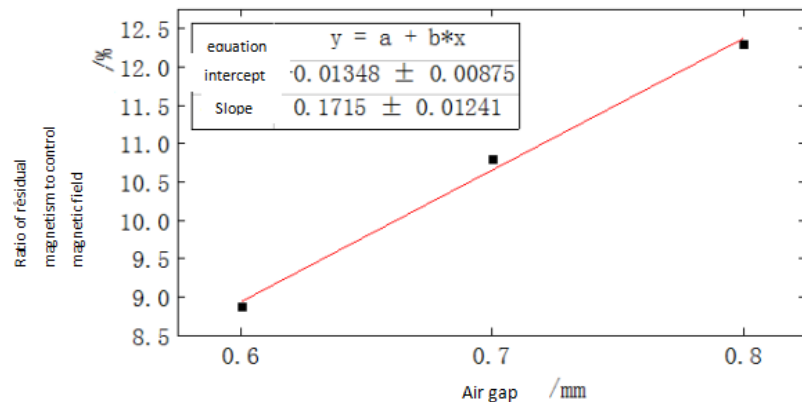


Fig. 15. The Ratio of Remanence to Control Magnetic Field at Different Air Gaps

The fitting curve obtained is  $y = -0.01348 + 0.1715x$ , thus it can be calculated that  $q_{0.4} = 5.48\%$  when the suspension control is not affected with the air gap of 0.4mm. Fig. 16 shows the simulation result of magnetic flux density between air gaps during normal suspension of axial magnetic bearing.

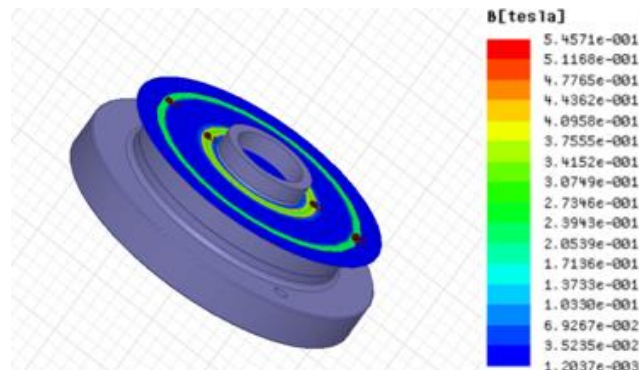


Fig. 16. Simulation result of magnetic flux density between stator and rotor air gaps

The magnetic flux intensities of the four points (m1.m2.m3.m4) between the air gaps are measured. As  $m1 = 329$  mT,  $m2 = 327$  mT,  $m3 = 219$  mT,  $m4 = 217$  mT are obtained respectively, the average value is taken.

$m = \frac{m_1 + m_2 + m_3 + m_4}{4} = 273\text{mT}$  is the magnetic flux density between the stator and rotor air gap during the stable suspension of the axial magnetic suspension rotor in an actual case. It can be seen from Table 1 that the remanence on the surface of the thrust plate is 18.7 mT when  $q = \frac{18.7}{273} \times 100\% = 6.85\% > q_{0.4} = 5.48\%$

Therefore, it is proved that the remanence has an impact on the suspension control of the magnetic suspension rotor, resulting in the unstable suspension of the axial magnetic suspension rotor. Using proportional-integral-derivative control algorithm to control the axial magnetic bearing of magnetic suspension rotor and debugging the proportional-integral-derivative control parameters, the effect of axial stable suspension are achieved finally. A group of data output from the axial sensor plotted into curves is as shown in Fig. 17.

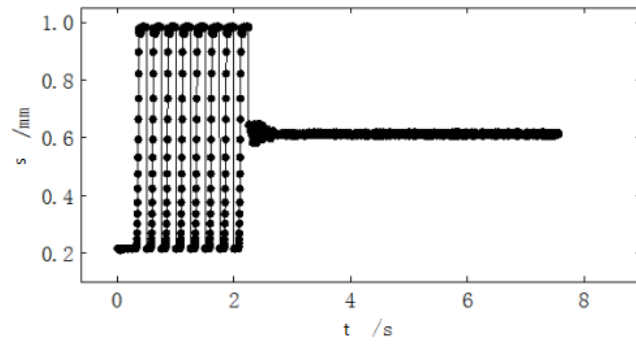


Fig. 17. Output displacement of the axial sensor during the stable suspension of magnetic suspension rotor

Fig. 18 shows that the magnetic suspension rotor has achieved stable suspension after a short period of floating. At this time, the current of front and rear coils of the axial electromagnet is shown in Fig. 18.

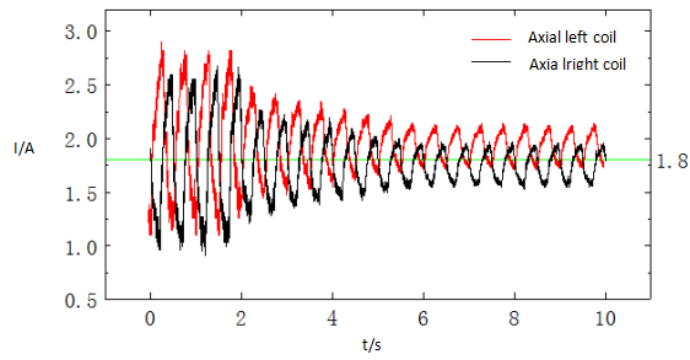


Fig. 18. Current of Axial Electromagnet Coils

Subsequently, Fig. 17 proves that the current of front and rear coils is basically the same from floating to stable suspension.

## 6. Conclusion

At present, researches on remanence mainly focuses on transformer core, the principle of remanence of transformer core and the analysis of the impact on the equipment have been mature, including how to reduce the impact of residual magnetic flux on the transformer [12-16], putting forward some preventive countermeasures for possible problems according to its characteristics [17-19]. But the working characteristics of magnetic suspension rotor are different from those of the transformer, the mechanism of remanence is not the same, the influence of residual magnetism on the control of magnetic suspension rotor and the results are different. At present, There are few theoretical studies on the influence of residual magnetism on magnetic suspension rotor control [20] made by experts and scholars.

In this paper, permanent magnet is used to simulate the remanence of magnetic bearing, and the correctness of remanence simulation is verified by experiment and simulation. Finally, the influence of remanence on the suspension control of magnetic suspension rotor is verified by experiment, which draws the following conclusions.

- (1) The hysteresis characteristic of magnetic material itself makes the magnetic bearing produce remanence after electrification, and remanence will have a certain influence on the suspension control of the magnetic suspension rotor.
- (2) When the ratio of the remanence between air gaps of magnetic bearing and the control magnetic field of magnetic bearing does not exceed the critical value, the remanence does not affect the stable suspension of the magnetic bearing; if the ratio exceeds the critical value, the remanence will affect the stable suspension.
- (3) Within the range of air gap studied herein, the air gap has an influence on the critical ratio of the remanence to the control magnetic field of magnetic bearing with the impact approximately linear.
- (4) The structure of magnetic suspension rotor also has an impact on the transfer of remanence.

## R E F E R E N C E S

- [1]. *Zhang Weiyu, Zhu Huangqiu, Yuan Ye. Study on Key Technologies and Applications of Magnetic Bearings. Transactions of China Electrotechnical Society, vol. 30, no. 12, 2015, pp. 12-20.*
- [2]. *Liu Zongchuan. Research of the Hysteresis model about ferromagnetic material. Master Thesis Guangxi University, 2006.*

- [3]. *Ge Wenqi, Wang Youhua, Chen Xueguang, et al.* Method to Measure and Weaken the Residual Flux of the Power Transformer Core. *Transactions of China Electrotechnical Society*, **vol. 30**, no. 16, 2015, pp. 10-16.
- [4]. *Feng Yuancheng, Zhang Han, et al.* The influence of transformer residual magnetism on equipment operation and its prevention. *Shanghai Electric Power*, **vol. 3**, no. 3, 2009, pp. 252-254.
- [5]. *Xing Yunmin, Luo Jian, Zhou Jianping, et al.* Estimation of Remanence in Transformer Core. *Power System Technology*, **vol. 2**, 2011, pp. 169-172.
- [6]. *Markus Püttner, Michael Rädler, Boris Unterer.* What Influence Does Residual Magnetism Have on the Transformer Core. *Transformers Magazine*, 2014.
- [7]. *Xu Xingshuai.* Probe into Detection Method of Residual Magnetism of Power Transformer Core. *Forum on Science and Technology in China*, **vol. 8**, 2016, pp. 97-97.
- [8]. *Hu Yefa.* Basic theory and application of magnetic bearings. China Machine Press, 2006.
- [9]. Technical Qualification Appraisal Committee for Non-destructive Testing Personnel of Weapon Industry. *Quick Check Manual of Magnetic Characteristic Curve of Common Steel*. China Machine Press, 2003.
- [10]. *Z. Yin, X. Kong, A. Chao, et al.* The Research of Co-simulation Control based on dSPACE and Siemens proportional-integral-derivative controlModule FM355C. *International Conference on Fluid Power & Mechatronics*, 2011.
- [11]. *Huang Yi.* Research on Control Method of Maglev Movement Platform Based on dSPACE. Central South University, 2009.
- [12]. *Andrzej Wilk, Michał Michna.* Simulation of the remanence influence on the transient states in a single-phase multiwinding transformer. *Archives of Electrical Engineering*, **vol. 66**, no. 1, 2017, pp. 41-54.
- [13]. *Yasin Zabihinia Gerdroodbari, Mahdi Davarpanah, Shahrokh Farhangi.* Remanent Flux Negative Effects on Transformer Diagnostic Test Results and a Novel Approach for Its Elimination. *IEEE Transactions on Power Delivery*, **vol. 33**, no. 6, 2018, pp. 2938-2945.
- [14]. *Wang Yang, Liu Zhizhen, Chen Hongxing.* Research on Residual Flux Prediction of the Transformer. *IEEE Transactions on Magnetics*, **vol. 53**, no. 6, 2017, pp. 6100304.1-6100304.4.
- [15]. *B.R. Chiheb, F. Farhani, A. Zaafouri, A. Chaari.* A novel adaptive control method for induction motor based on Backstepping approach using dSpace DS 1104 control board. *Mechanical Systems & Signal Processing*, **vol. 100**, 2018, pp. 466-481.
- [16]. *J. Li, Z. Li, X. Zhong, et al.* Remanence detection and low-frequency degaussing for power transformers based on modified J-A model. *2015 IEEE International Magnetics Conference, INTERMAG 2015*, 2015.
- [17]. *Bai Baodong, Chen Zhiwei, Chen Dezhi.* DC Bias Elimination and Integrated Magnetic Technology in Power Transformer. *IEEE Transactions on Magnetics*, **vol. 51**, no. 11, 2015, pp. 8401304.1-8401304.4.
- [18]. *Kiani, Mandi, Salarieh, Hassan, Alasty, Aria, et al.* Hybrid control of a three-pole active magnetic bearing. *Mechatronics: The Science of Intelligent Machines*, **vol. 39**, 2016, pp. 28-41.
- [19]. *B. Kovac, F. de León, D. Czarkowski, Z. Zabar, L. Birenbaum*, “Mitigation of inrush currents in network transformers by reducing the residual flux with an ultra-low-frequency power source”, *IEEE Trans. Power Del.*, **vol. 26**, no. 3, Jul. 2011, pp. 1563-1570.
- [20]. *P.V.S. Sobhan, G.V.N. Kumar, J. Amarnath.* Rotor levitation by active magnetic bearings using fuzzy logic controller. *Proc. Int. Conf. Ind. Electron. Control Robotics (IECR)*, 2010.